

Title: Thermal Expansion of Thin Films: A Review

Author: Ernest G. Wolff

## **ABSTRACT**

Thin films, tapes, foils, laminae, weaves and cloths, coatings, and planar components and devices are increasingly required to maintain dimensional stability during changing environmental conditions. The technology for the measurement of thin film coefficients of thermal expansion (CTE) is scattered among numerous disciplines. This review presents many of the diverse approaches that have been employed and discusses the major techniques that have been used including laser pulse, capacitance, X-ray diffraction, differential curvature, photothermal, ellipsometry, and various interferometers such as Fabry-Perot, Fizeau and Michelson. Some novel methods such as the use of electron reflectance, ion channeling and scanning thermal microscopy were also employed. In most cases, metal, ceramic or polymeric films less than 10 microns thick were deposited on Si, glass, or silica substrates. Some general observations on the behavior of thin films relative to bulk materials are also reviewed.

## **INTRODUCTION**

Many groups have worked on CTE of thin films, principally in the US, Germany, Japan, the former USSR, and about 10 other countries. Table I lists the major laboratories, about half being universities. This review is not claimed to be complete, although it is the product of several computerized literature searches.

Thin films are principally characterized by their geometry which distinguishes deviations from bulk behavior in terms of sample support, edge/end effects, thermal equilibration, residual stresses, additional anisotropy, surface tension/energy and many unique atomic or molecular arrangements. As a result, CTE data are often difficult to generalize to other films of the same material.

TABLE II - TEST METHODS FOR CTE OF THIN FILMS

	Figures	References
<b>INTERFEROMETRIC METHODS</b>		
Fabry-Perot	(2)	[4,40]
Fizeau		[8,27,31,51]
Michelson	(1,3,4,5,7)	[6,8,41]
General Interferometry		[8,23,28,41]
Fiber Optics	(6,8)	[2]
<b>NON-INTERFEROMETRIC OPTICAL METHODS</b>		
Ellipsometry		[25,30]
Optical Lever	(10,11)	[11,26,29,33,45]
Laser Transmission		[52]
Photothermal		[13]
Microscopy		[21]
Scanning Tunneling Microscope		[6,34]
<b>DIFFRACTION</b>		
X-ray		[22,24,53]
Optical		[1]
Electron		[19]
Thermal He		[44]
<b>NON-OPTICAL METHODS</b>		
Capacitance	(12-15)	[4,10,17,18,40]
Curvature	(9-11)	[5,8,9,15,24,29,32,45]
Volumetric	(16)	[12]
TMA		[4]
Ion Channeling		[37]
Microbalance		[14]
Glass Helix Rotation		[38]

$$\sigma_f = \frac{1}{6} \frac{E_s}{(1 - \nu_s)} \frac{t_s^2}{t_f} \left[ \frac{1}{R_f} - \frac{1}{R_o} \right] \quad (1)$$

$R_o$  and  $R_f$  are the radii of curvature of the substrate before and after deposition.  $\sigma_f$  is the biaxial stress in the film on a substrate with Young's modulus  $E_s$  and Poisson's ratio  $\nu_s$ . Thermal stresses arise when the system is baked at a temperature  $T_b$  (e.g., to cure the polymeric film) and cooled to the measurement temperature  $T$  [47]

$$\sigma_T = \frac{E_f}{(1 - \nu_f)} (\alpha_f - \alpha_s) (T_b - T) \quad (2)$$

One assumes that stresses change reversibly between  $T_b$  and  $T$  and that all stresses are due to the (in-plane) CTE mismatch. Thus one may combine Equations (1) and (2) [8] to obtain

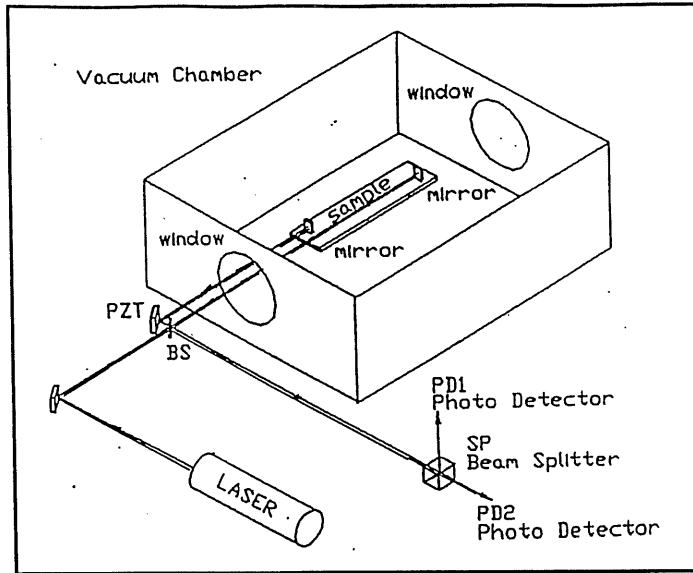


Figure 1. Horizontal LASER Interferometer

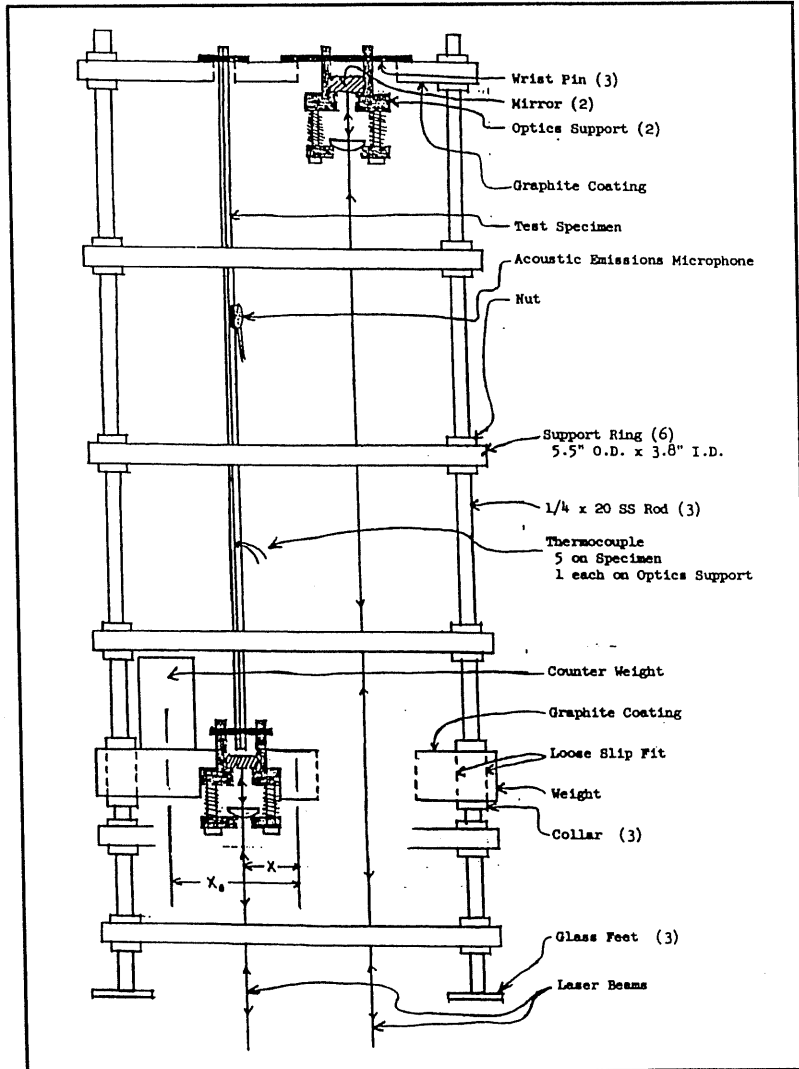


Figure 2. Michelson Interferometer for Fibers, Strips, Etc.

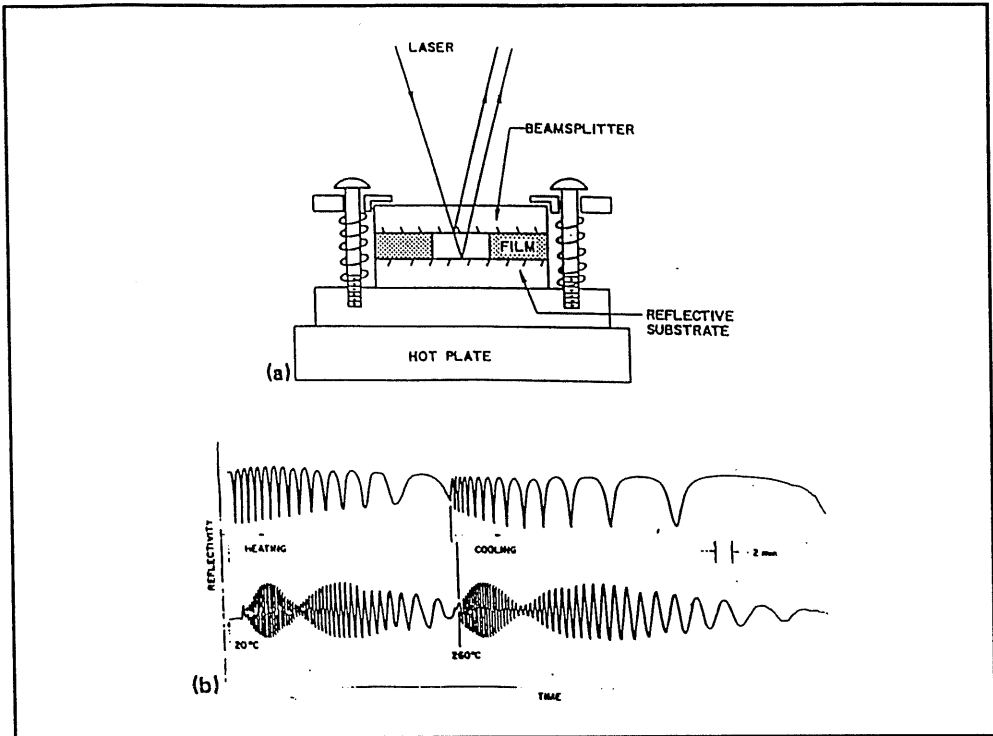


Figure 3. (a) Fabry-Perot Laser Interferometer [57]. (b) Reflectivity as a Function of Time for a 5-Mil-Thick Kapton Film (Top Trace) and a Sapphire Thermometer (Bottom Trace) During Thermal Cycling Between 20 and 260°C [4].

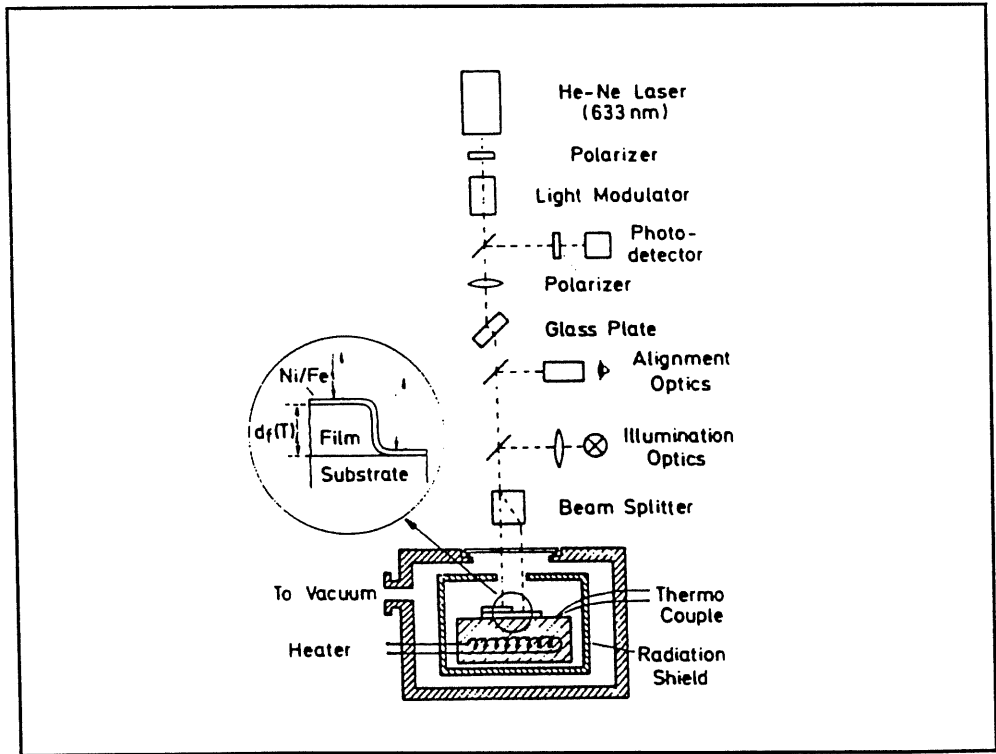


Figure 4. Two-Beam Laser Interferometer for Measuring the Change in Film Thickness  $\Delta d_f$  as a Function of Temperature. The laser beams are scanned at the sample surface via computer-controlled tilting of the glass plate. Vacuum box and radiation shield serve to minimize the heating of temperature-sensitive parts (e.g., beam splitter). [8]

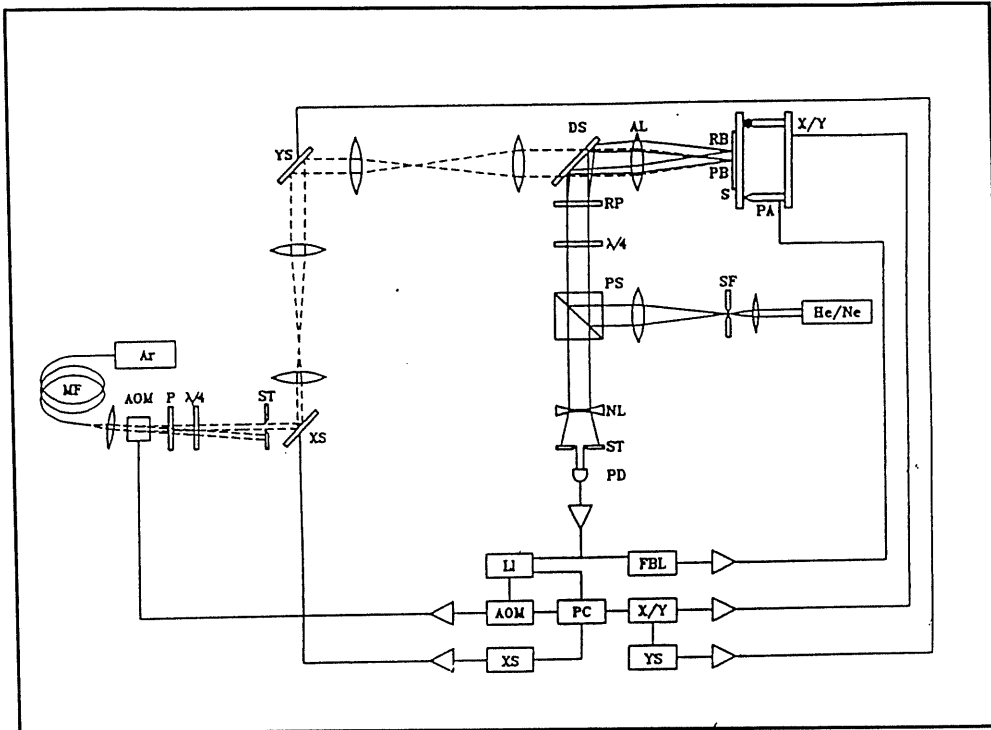


Figure 5. Photo-Thermal Laser Interferometer Set-Up Used for the Locally Resolved Investigation of the Thermal Expansion of Laser Heated Samples [6].

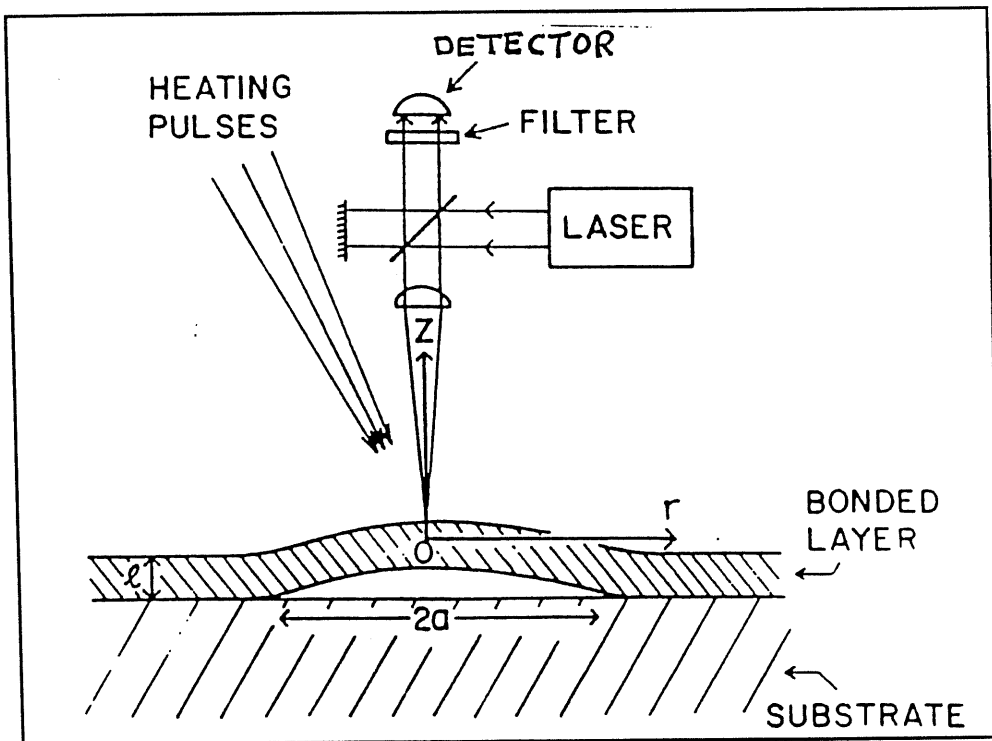


Figure 6. Basic Principle of the Method for Detecting an Unbonded Area of Size  $2a$  with a Layer Thickness  $l$ , and Axes of the Theoretical Model. The temperature gradients induced by the surface-heating pulse produce the thermoelastic bending of the unbonded layer, and its vertical displacement is measured by a focused laser interferometer [41].

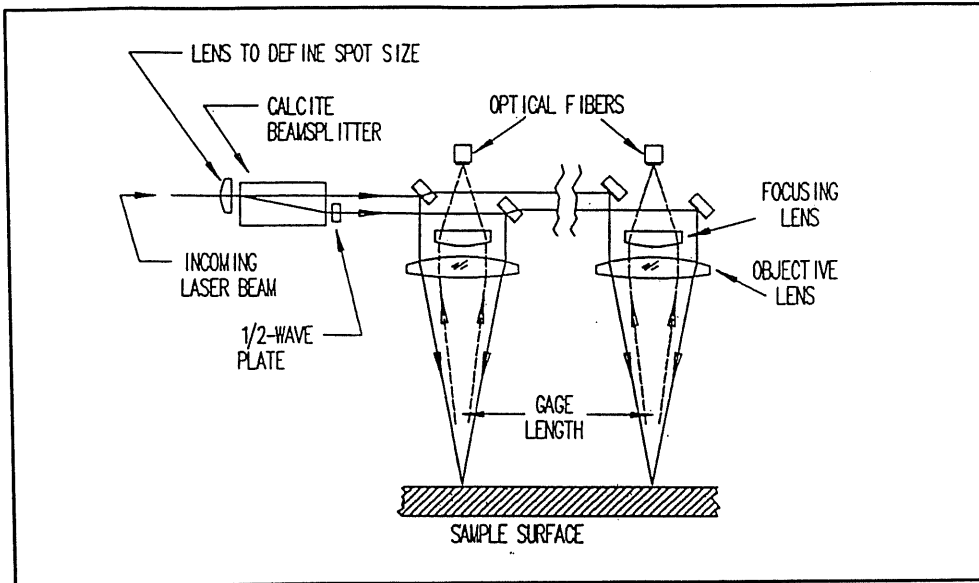


Figure 7. Optical Layout of Extensometer [55]

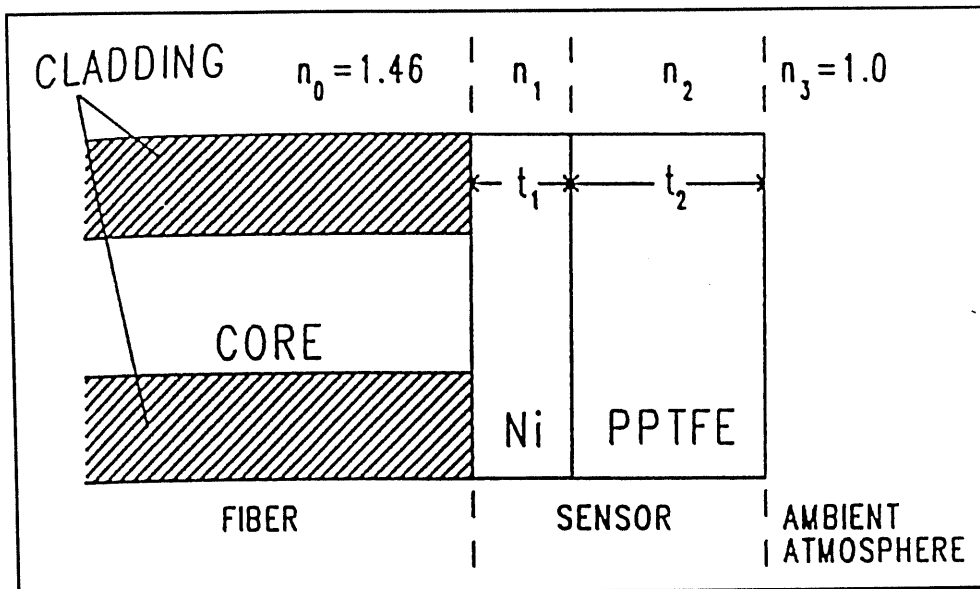


Figure 8. Schematic Diagram of the Microinterferometer on the End of a Multimode Optical Fiber. The complex index of refraction of Ni is  $2.59-4.55i$  at 850 nm and  $t_1$  is 100 Å [2].

$$\frac{1}{R_f} = \frac{6 E_f t_f (1 - \nu_s)}{E_s t_s^2 (1 - \nu_f)} (\alpha_f - \alpha_s) (T_b - T) + \frac{1}{R_o} \quad (3)$$

and  $\alpha_f$  (the film in-plane CTE) can be derived from the slope of a plot of  $R_f$  vs.  $T$ . Such use of curvature from biaxial stress states was used in references [8,9,11,14,16,26,33,35,43]. A number of auxiliary techniques can be used to detect the curvature, such as Fizeau interferometry [8], optical flats (Figure 9, [15]), Newton's

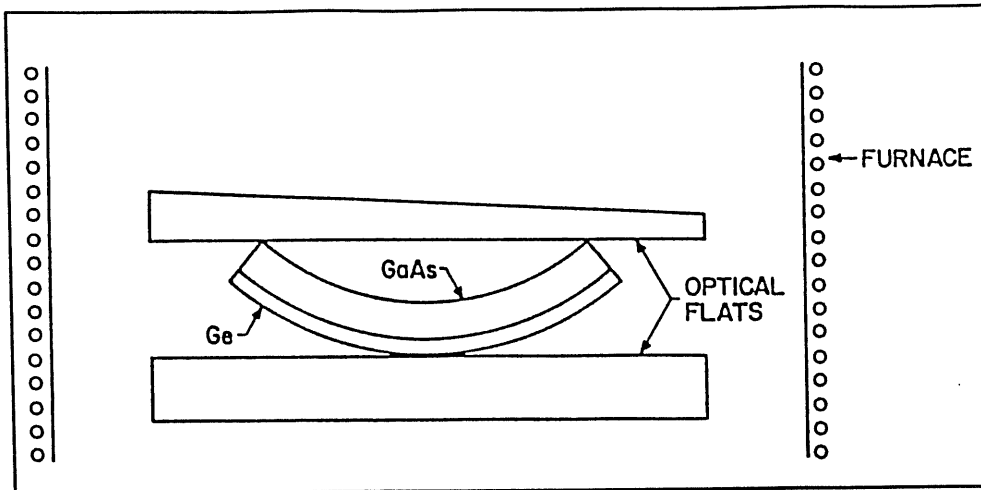


Figure 9. Arrangement of Thin-Layer Couple and Optical Flats in Furnace [15]

rings [16] or optical levers (Figures 10 [26] and 11 [11]). By using films deposited on two different substrates one can solve for  $\alpha_f$  and  $\{E/(1-\nu)\}_f$  [33,35,43]. The technique may also be applied to a three layer system, as when a diffusion barrier such as W is placed between Au and Si [35]. Since this technique depends on good adhesion of the film to the substrate, surface factors can play an important role. The film stresses developed were found to be very sensitive to cleaning techniques of the substrate (Ni) prior to (e-beam) deposition of the (Ni) films [14]. Most of the workers dealing with this technique have major concerns with the residual stress state of the film.

## CAPACITANCE METHODS FOR Z-DIRECTION

The general theory is outlined as follows: If  $d$  is the film thickness, the capacity of the dilatometer (e.g., Figure 12) is

$$C = \epsilon_0 A/d \quad (4)$$

where  $\epsilon_0$  is the permittivity of a vacuum. Differentiating

$$(\Delta d)/d = -(\Delta C)/C = (\text{CTE}) * \Delta T \quad (5)$$

A correction is needed for lateral expansion of the film/substrate combination [17,18]. Refinements include weights to maintain film/electrode contact and specially cut samples to minimize sample dielectric behavior (Figures 13,14) [4,40], counterweights to avoid pressure on the films (Figure 15) [10], and minimal spacing to avoid the need for guard rings [17,18].

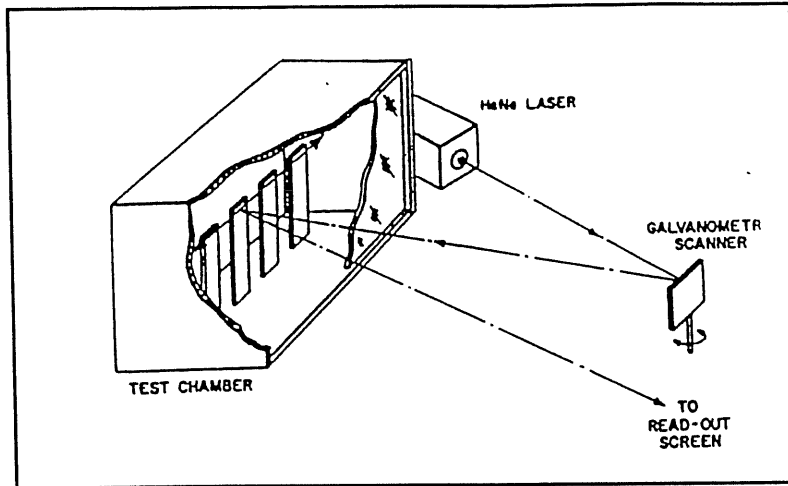


Figure 10. A Schematic View of the Experimental Arrangement [26]

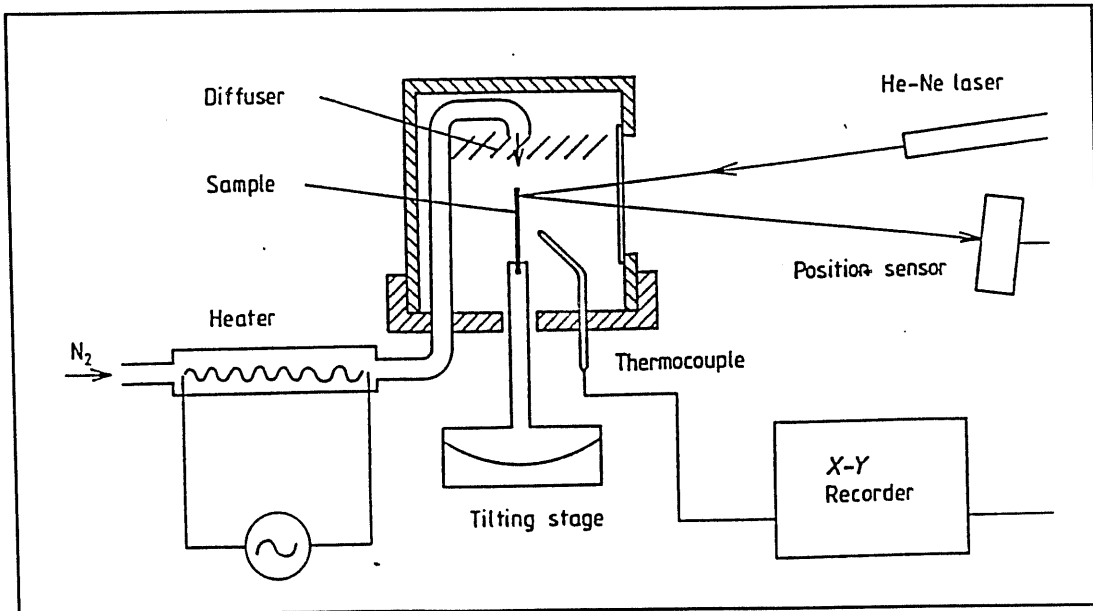


Figure 11. Experimental Setup for Measuring the Expansion of a Thin Film [11]

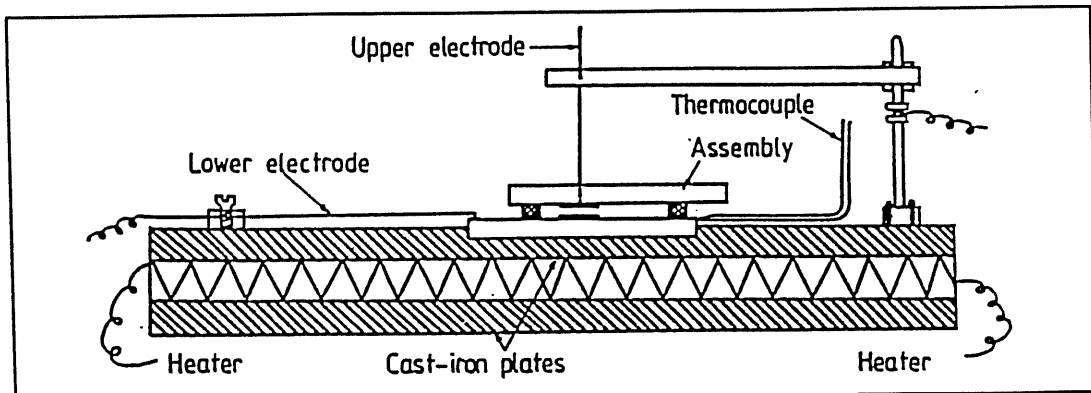


Figure 12. Dilatometer Cell Showing the Assembly of the Measurement of the Thermal Expansion of Thin Films [18]



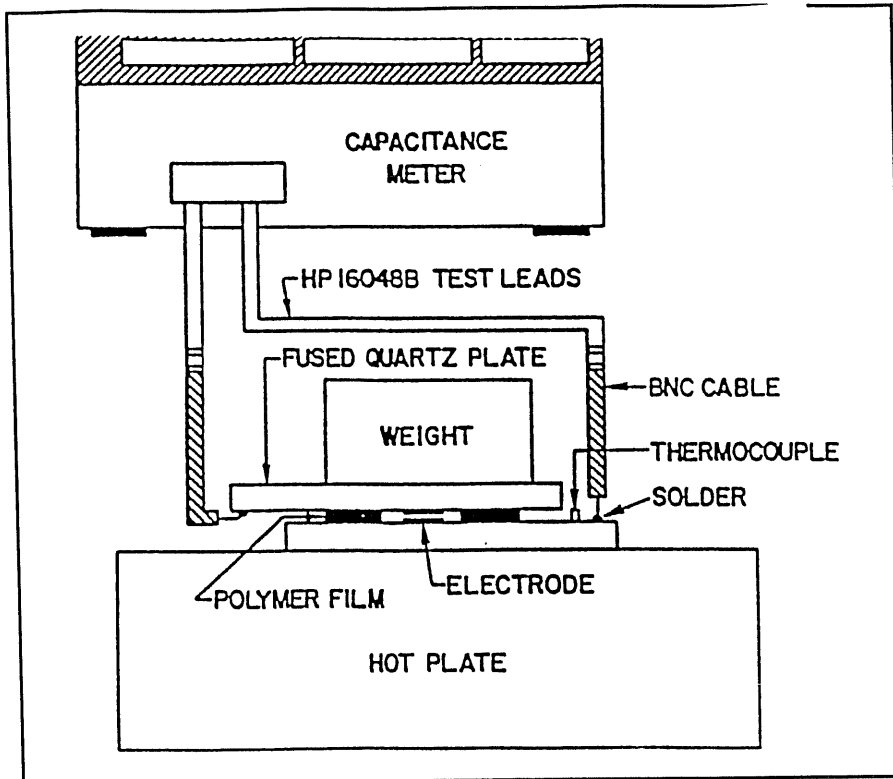


Figure 13. Capacitance Change Apparatus [40]

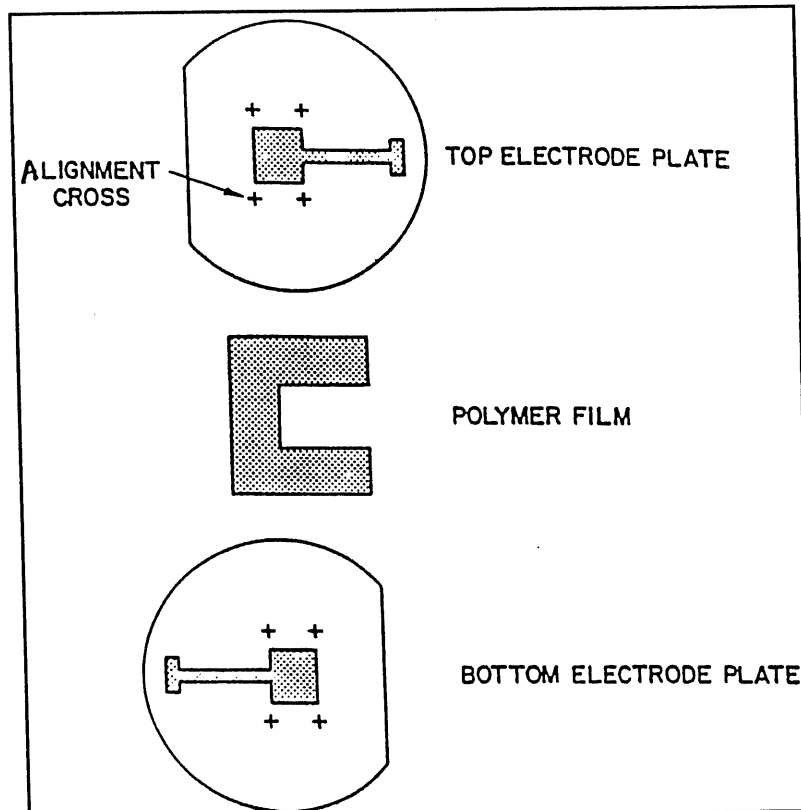


Figure 14. Plan View of Capacitor for CTE Measurements [4,40]

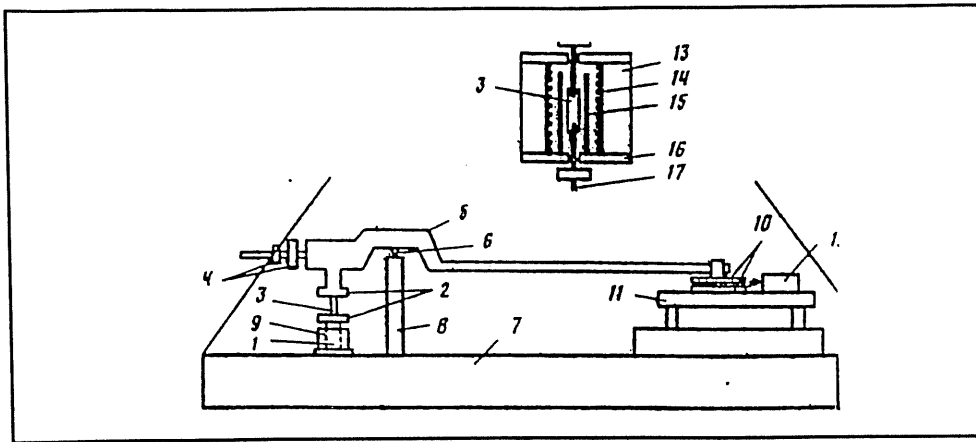


Figure 15. Dilatometer: 1) quartz plate; 2) specimen clamp; 3) specimen; 4) counterweights; 5) beam; 6) quartz prism; 7) base; 8) post; 9) metal plates; 10) measuring capacitor; 11) adjustable platform; 12) generator; 13) housing of microfurnace; 14) heating element; 15) metal foil; 16) heat-insulating covers; 17) quartz filaments [10]

## MISCELLANEOUS TEST METHODS

Figure 16 represents a method to obtain the volumetric CTE (XYZ), a technique normally reserved for larger samples.

Laser pulse heating produces nonsynchronous changes of temperature and thermal expansion; the temperature rises faster than the expansion can follow (Figure 17, [1]). Another aspect of pulse heating is localized absorption of energy, expansion and possibly separation of the film from the substrate. In this case one has the complex photothermal surface-deformation technique from which film/substrate thermal expansion coefficients differences could be inferred [13]. Laser pulse heating of unbonded areas in thin films, coupled with interferometric measurement of the vertical displacement [41] could in principle be applied to the determination of thin film CTE. However, this technique is considered more suitable to NDT inspection than to CTE determination because of the analytical complexity of separating the combined effects of  $\alpha_z$ ,  $\alpha_{xy}$ , the temperature distribution and the geometry of the disbond.

Multiple test techniques were used and compared in References [4,6,40]. Photo-acoustic, photothermal, thermal imaging and thermoacoustic techniques are compared in [42]. While written with a view to NDT, the comments are also pertinent to the use of these techniques for CTE measurement.

## MEASUREMENT RESULTS ON THIN FILMS

Elsner et al. [8] found that polyimide (PI) films deposited on Si wafers and also quartz plates showed an XY-CTE of only  $9 \times 10^{-6}/^{\circ}\text{C}$  while the Z-direction CTE was about  $110 \times 10^{-6}/^{\circ}\text{C}$ . The former is about 3X too small; the latter 3X larger than the normal bulk value of  $30 \times 10^{-6}/^{\circ}\text{C}$ . While adhesion to the small CTE substrate partially explains the low lateral value, in-plane orientational changes of the molecular chain structures due to the mode of deposition (spin coating) are claimed to account for the anisotropy. Similar results were found for other polyimide films; e.g., for

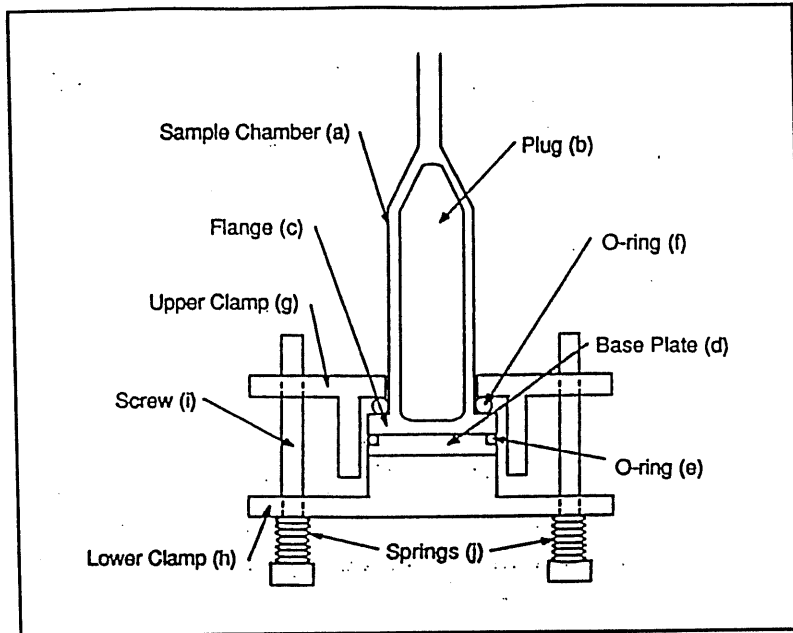


Figure 16. Detailed Diagram of the Thin Film Dilatometer [12]

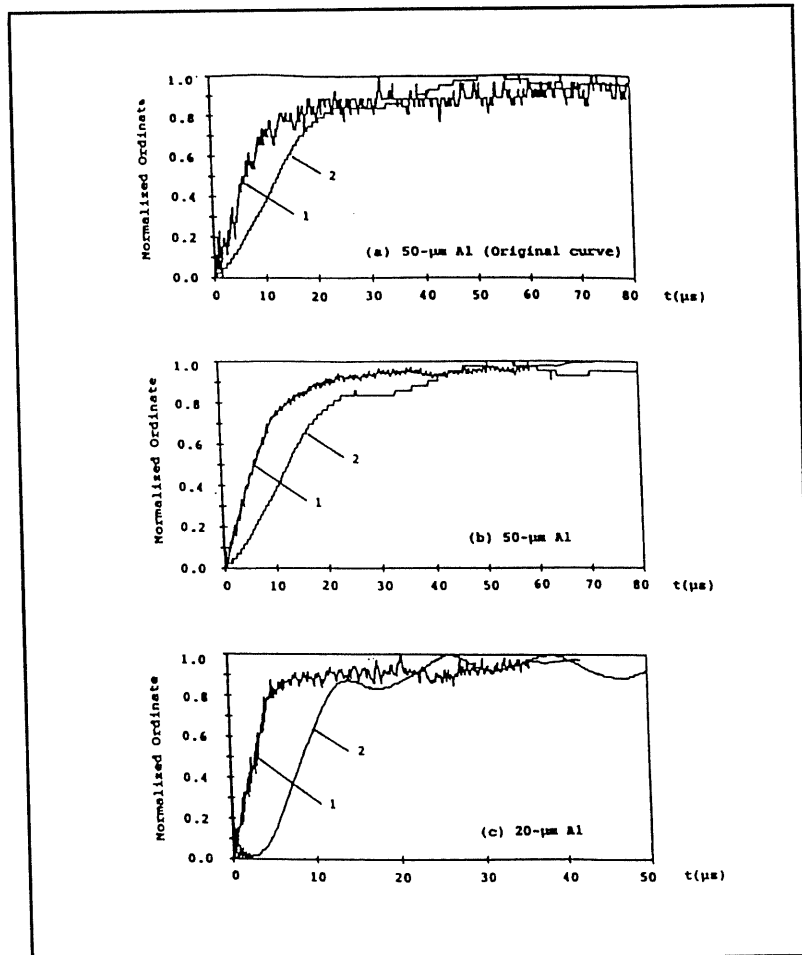


Figure 17. Comparison of Temperature Rise and Thermal-Expansion Curves (1 - temperature rise, 2- thermal expansion) [1]

Kapton,  $\alpha_z$  was about 2.4 times  $\alpha_{xy}$  [40]. Other work suggests that the polyimide CTE increases as film thickness increases on account of lesser orientational effects caused by the substrate [43].

Considerable work has been done on silicide films [9,24,29]. The effects of thermal cycling, film crystallization, annealing and stress induced interactions with a substrate is discussed in [9] to help explain in-plane CTE results on W-Si-N films. Pure W films were found to exhibit bulk tungsten properties [9]. Thin films of W and Au also showed bulk CTE values in [35]. But pure metals can still show deviations from bulk values when in a thin film form. Iron (and also Cr, V, Co, Cr) films (on glass, SiO<sub>2</sub> substrates) showed bulk CTE values but lowered Young's moduli (Figure 18 [11]), attributed to oriented crystallites. The latter effect was also noted for Au films [35]. Annealing of Au films lowered their biaxial Young's modulus, again attributed to grain growth.

Amorphous and crystalline materials, for other factors being equal, should have similar values of CTE [50]. Thus, when a higher CTE was found for amorphous Si films than for crystalline Si [26], it was attributed to the absorbed hydrogen from the glow-discharge enhanced CVD process. A similar effect was noted for hydrogenated amorphous germanium films (Figure 19 [28]) after reactive sputtering. (The effect of further nitrogen to Ge-H films is to decrease the CTE (Figure 20 [26,33]). Thus the fabrication method is another factor to consider when evaluating thin film CTEs.

In ferroelectric thin films, thermal expansion measurements are affected by strains due to piezoelectric, pyroelectric and/or electrostrictive forces [17,48]. Thermal expansion mismatches between film and substrate can also cause faceting and cleavage cracks in films [22]. Figures 21-23 show further results from the studies reviewed.

An unusual phenomenon gives rise to oscillations of CTE with temperature. Nedorezov [58] proposed a theory based on the non-equidistance of the quantum energy levels of the carriers in thin films. The theory was tested by Aliev and others [38] on 500 Å CuS films. Figure 24 shows CTE oscillations as a function of temperature.

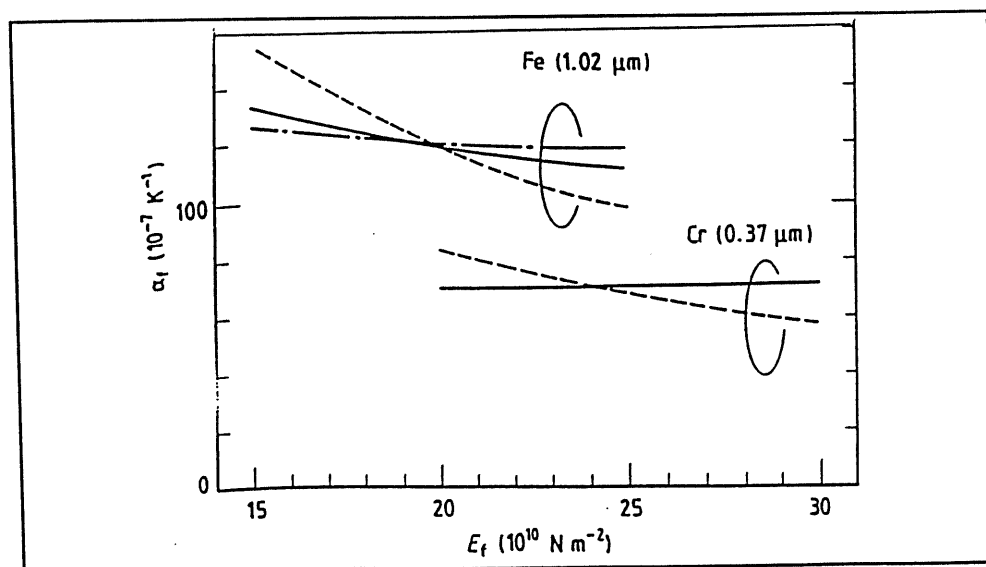


Figure 18. Thermal Expansion Coefficients of Iron and Chromium Films on Various Substrates.  $\alpha_f$  is plotted as a function of the parameter  $E_f$ . — PEG<sup>R</sup> ( $\alpha_s = 105 \times 10^{-7} \text{ K}^{-1}$ ), — BK-1<sup>R</sup> ( $\alpha_s = 87 \times 10^{-7} \text{ K}^{-1}$ ), — — — SiO<sub>2</sub> ( $\alpha_s = 4 \times 10^{-7} \text{ K}^{-1}$ ) [11]

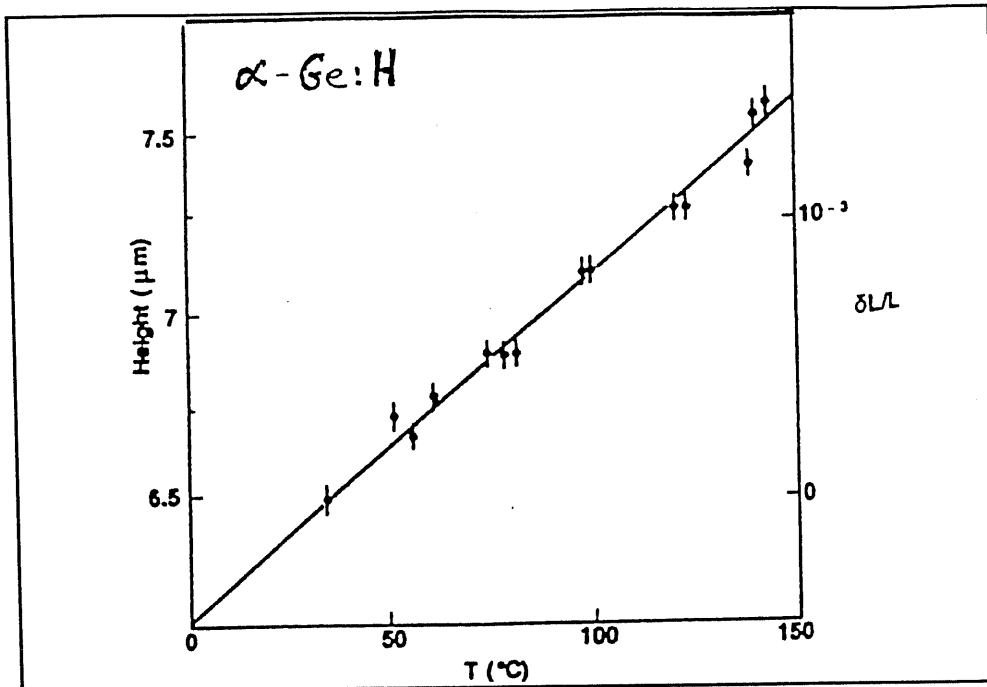


Figure 19. Film Height Derived Using Eq. (2) and the Distance Between the 23rd Fringe Pair (counted from the Substrate-Film Contact) Plotted Against Temperature [28]

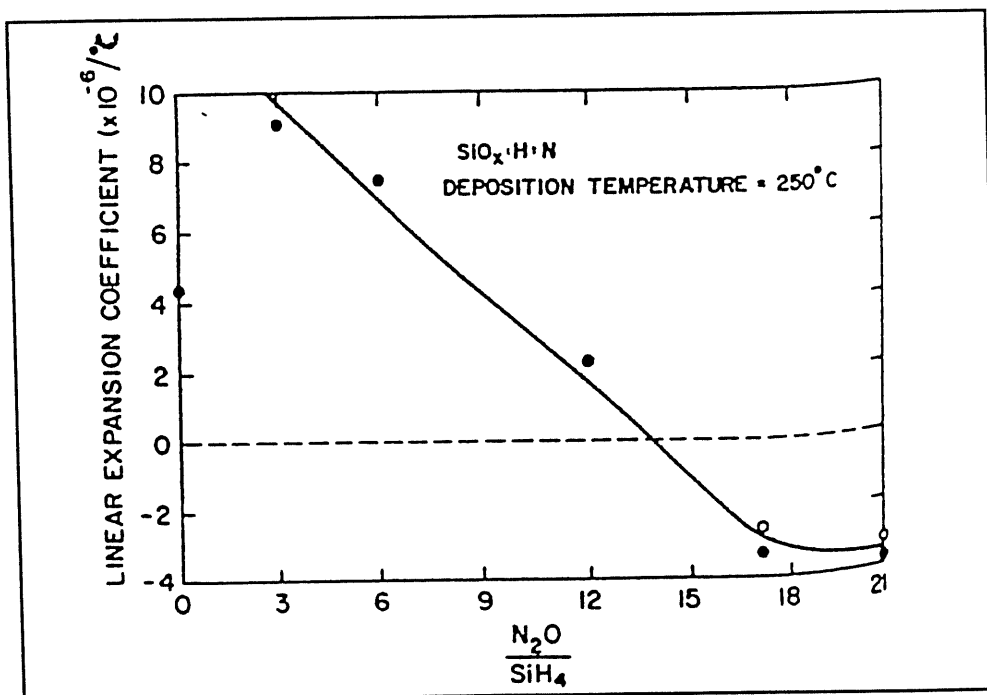


Figure 20. Thermal Expansion Coefficient of PECVD  $\text{SiO}_x$  Films, Deposited at  $250^{\circ}\text{C}$ , as a Function of the precursor Gas Ratio [26]

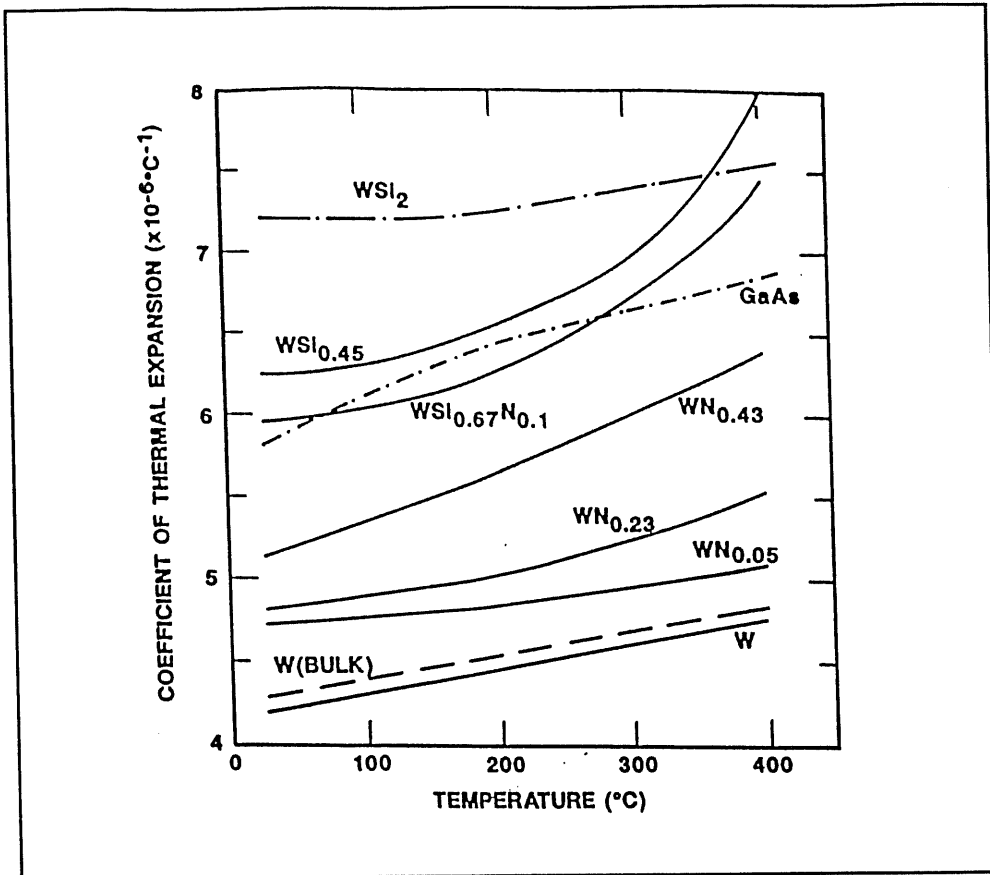


Figure 21. Temperature Dependence of the Coefficients of Thermal Expansion of the W-Based Films in Comparison with the Data for Polycrystalline Bulk W and  $\text{WSi}_2$ , and Single Crystal (100) GaAs [9]

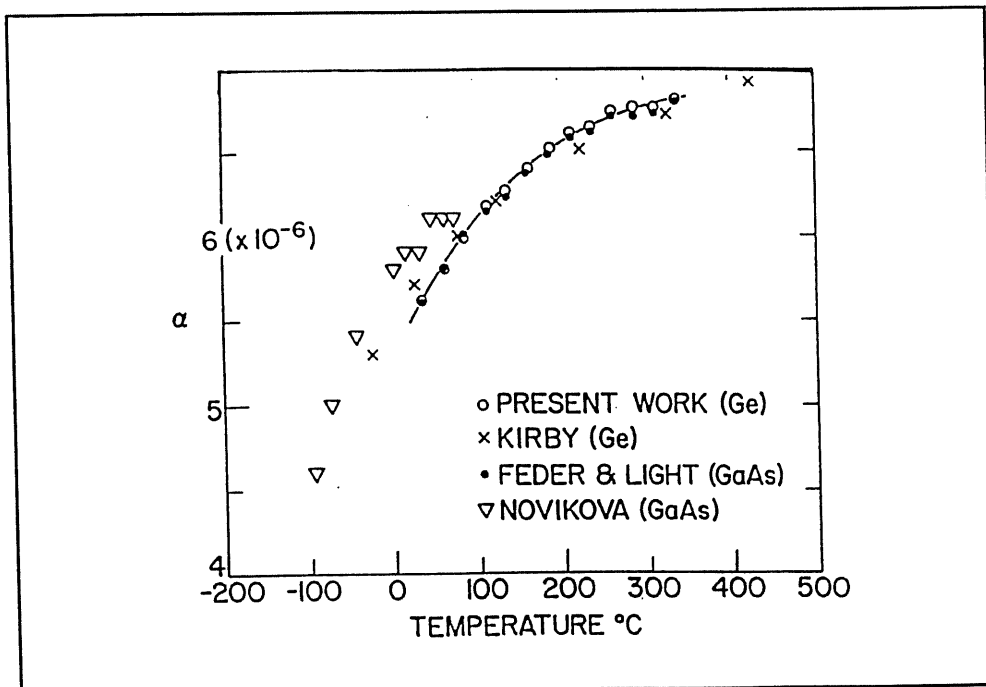


Figure 22. Thermal Coefficient of Expansion ( $\alpha$ ) as a Function of Temperature [15]

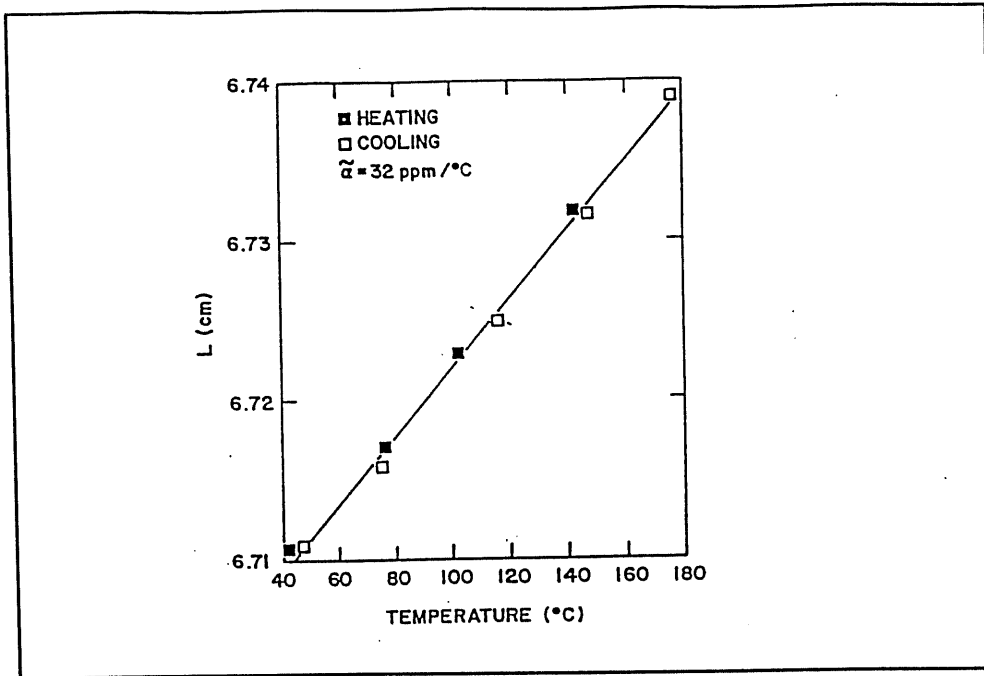


Figure 23. In-Plane Length vs Temperature Data for a 5-Mil-Thick Kapton Film. Experiment (squares); fit (solid line) [4]

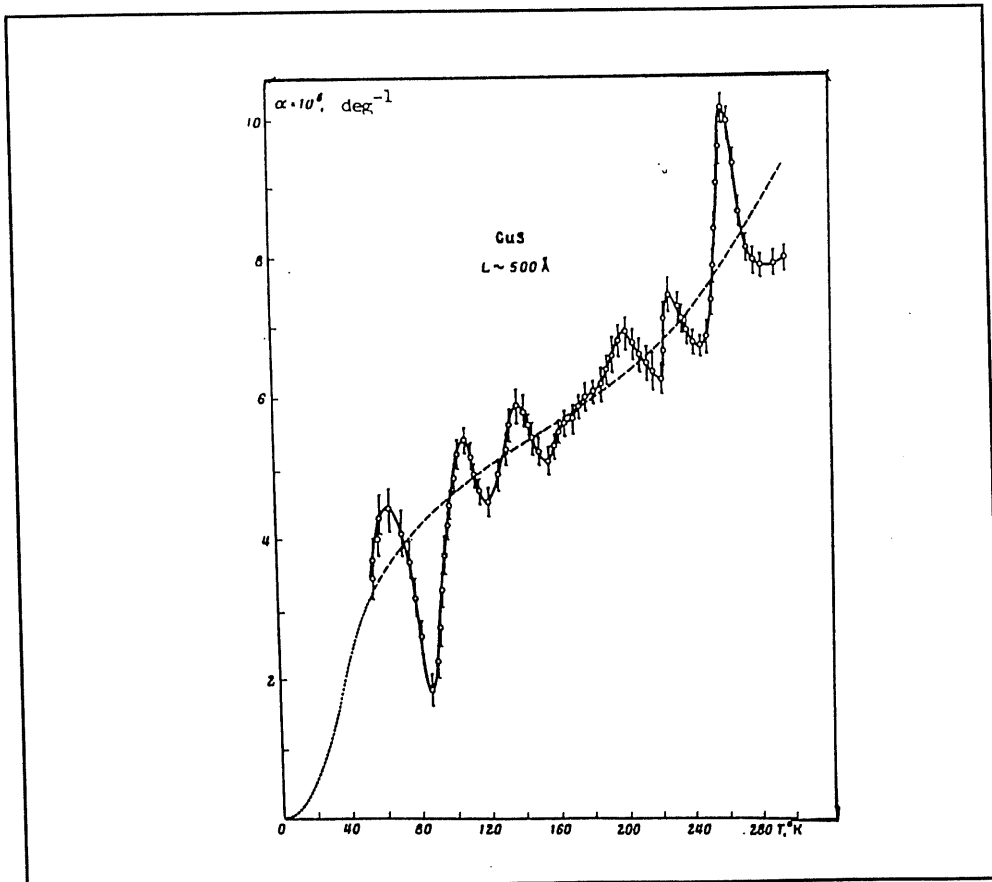


Figure 24. Temperature Dependence of the Coefficient of linear Thermal Expansion of Semiconducting CuS Film 500 Å Thick [38]

## CONCLUSIONS

Numerous techniques to measure CTE exist, principally interferometric, curvature, capacitance, and diffraction methods. High speed techniques may decouple thermal and expansion behavior. Major work reported is from microelectronics oriented laboratories. Films behave differently than bulk materials; for example, for polymers,  $Z\text{-CTE} > XY\text{-CTE}$  while the Young's modulus of films is often less than  $E$  (bulk).

Factors which influence the CTE of thin films include fabrication (or deposition) parameters, absorbed gases, moisture absorption and residual stresses. Residual stress analysis was reviewed by IBM workers [53]. Intrinsic parameters imply the structure of the film itself, including impurities or voids. Extrinsic effects are mainly due to the substrate, such as interdiffusion, interlayers, epitaxy or orientational effects. Surface cleanliness, adhesion and the CTE of the substrate affect the film behavior. Thermal cycling can influence recrystallization, annealing and cracking or faceting of the film. For some materials, piezoelectric, pyroelectric and electrostrictive effects are important.

Although there are numerous techniques available for the measurement of CTE, there have been few attempts to cover a broad temperature range with a variety of thin film materials. Few graphs of thermal strain versus temperature were found. This suggests a need to develop a more general data base. Most of the work to date has followed the sequence of measurement and then attempts to rationalize the results in terms of residual stresses, epitaxy, etc. The general state of the art requires further study with predictive models and their verification.

## REFERENCES

1. Tang, D.W., B.L. Zhou, H. Cao and G.H. He, 1991. *Applied Physics Letters*, 59(24):3113-3114.
2. Butler, M.A., R.J. Buss and A. Galuska, 1991. *J. Applied Physics*, 70(4):2326-2332.
3. Tye, R.P. and A. Maesono, 1991. *Electronic Packaging Materials Science V. Symposium*, pp. XIII +455, 169-75.
4. Tong, H.M., H.K.D. Hsuen, K.L. Saenger and G.W. Su, 1991. *Review of Scientific Instruments*, 62(2):422-430.
5. Nicholson, E.D. and J.E. Field, 1994. *Journal of Hard Materials*, 5(3):89-132.
6. Oesterschulze, E., L. Hadjiiski, M. Stopka and R. Kassing, 1995. *Materials Science Forum* (Switzerland), 185-188:43-52.
7. Brueckner, W., 1995. *Physica Status Solidi A*, 148(2):K89-91.
8. Elsner, G., J. Kempf, J.W. Bartha and H.H. Wagner, 1990. *Thin Solid Films*, 185(1):189-197.
9. Lahav, A., K.A. Grim, and I.A. Blech, 1990. *Journal of Applied Physics*, 67(2):734-738.
10. Bashirov, V.Z. and A.P. Kal'yanov, 1989. *Pribory i Tekhnika Eksperimenta*, 32(2):223-224; *Instruments and Experimental Techniques*, 32(2) Pt.2: 509-511.
11. Iwasaki, Y., M. Kaneko, K. Hayashi, Y. Ochiai, M. Hayakawa and K. Aso, 1989. *Journal of Physics E (Scientific Instruments)*, 22(7):498-502.



12. Parsons, A.T. and C.M. Balik, 1989. *Review of Scientific Instruments*, 60(2):219-221.
13. Welsch, E., H.G. Walther, P. Eckardt and T. Lan, 1988. *Canadian Journal of Physics*, 66(7):638-644.
14. Springer, R.W. and R.W. Hoffman, 1973. *Journal of Vacuum Science and Technology*, 10(1):238-240
15. Feder, R., and T.B. Light, 1972. *Journal of Applied Physics*, 43 Pt. 4(7):3114-3117.
16. Sunami, H., Y. Itoh and K. Sato, 1970. *Journal of Applied Physics*, 41(13):5115-5117.
17. Sao, G.D. and H.V. Tiwary, 1982. *Journal of Applied Physics*, 53(4):3040-3043.
18. Tiwary, H.V. and G.D. Sao, 1981. *Journal of Physics E (Scientific Instruments)*, 14(12):1378-1380.
19. Pugachev, A.T. and N.P. Churakova, 1980. *Zavodskaya Laboratoriya*, 46(8):813-815.
20. Parakh, M., 1980. *IBM Technical Disclosure Bulletin*, 22(88):3865-3867.
21. Kirillov, V.N., Z.P. Ablekova, G.K. Gudkova and Ya.A. Abeliiov, 1978. *Zavodskaya Laboratoriya*, 44(12):1505-1506; *Industrial Laboratory*, 44(12):1715-1716.
22. Sugii, K. and S. Kondo, 1979. *Journal of Crystal Growth*, 46(5):607-614.
23. Oesterschulze, E., M. Stopka, M. Tochtrop-Mayr, K. Masseli and R. Kassing, 1993. *Applied Surface Science (Netherlands)*, 69(1-4):65-68.
24. Jongste, J.F., O.B. Loopstra, G.C.A.M. Janssen and S. Radelaar, 1993. *Journal of Applied Physics*, 73(6):2816-2820.
25. Beaucage, G., R. Composto and R.S. Stein, 1993. *Journal of Polymer Science, Part B, (Polymer Physics)*, 31(3):319-326.
26. Jenson, F., M.A. Machonkin, N. Palmieri and O. Kuhman, 1987. *Journal of Applied Physics*, 62(12):4732-4736.
27. Bartholemew, C., 1986. *Journal of Physics E (Scientific Instruments)*, 19(3):236 (1986).
28. Persans, P.D. and A.F. Ruppert, 1986. *Journal of Applied Physics* 59(1):271-273.
29. Retajczyk, T.F. and A.K. Sinha, 1980. *Thin Solid Films*, 70:241-247.
30. Guo, S., I. Lundstrom and H. Arwin, 1996. *Applied Physics Letters*, 68(14):1910-1912.
31. Bailey, A.C. and B. Yates, 1970. *Journal of Applied Physics*, 41(13):5088-5091.
32. Stoney, G.G., 1909. *Proceedings of the Royal Society (London)*, A82:172.
33. Lacerda, R.G., M.M. Lima, J. Vilcarromero, F.C. Marques, 1996. *AIP Conference Proceedings*, 378:315-318.
34. Stopka, M., E. Oesterschulze, J. Schulte and R. Kassing, 1994. *Materials Science & Technology B (Switzerland) (Solid State Materials for Advanced Technology)*, B24(1-3):226-228.
35. Jou, J-H., Chien-Neng Liao and Ke-Wei Jou, 1994. *Thin Solid Films*, 238(1):70-72.
36. Schwarzer, N., F. Richter and G. Hecht, 1993. *Surface Coatings Journal (Switzerland) Surface and Coatings Technology*, 60(1-3):396-400.

37. Hashimoto, S., J.-L. Peng, L.J. Schowalter and W.M. Gibson, 1985. *Proceedings 1st International Symposium on Silicon Molecular Beam Epitaxy*, Toronto, pp. ix+455:304-310.
38. Aliev, F.Yu., F.R. Godzhaev, I.G. Kerimov and E.S. Krupnikov, 1972. *JETP Letters*, 15:16-18.
39. Shmatok, Yu.I. and M.A. Markman, 1978. *Instruments and Experimental Techniques*, 21(1):253-254.
40. Tong, H.M., K.L.Slaenger and G.W. Su, 1993. *Polymer Engineering and Science*, 33(22):1502-1506.
41. Rousset, G. and L. Bertrand, 1985. *Journal of Applied Physics*, 57(9):4396-4405.
42. McDonald, F.A., 1986. *Canadian Journal of Physics*, 64:1023-1029.
43. Jou, J-H. and L-J. Chen, 1991. *Applied Physics Letters*, 59(1):46-47.
44. Zeppenfeld, P., 1989. Report # Jul-2305, Kernforschungsanlage, Julich:166.
45. Sinha, A.K., H.J. Levinstein and T.E. Smith, 1978. *Journal of Applied Physics*, 49(4):2423-2426.
46. Thomas, R.E., 1970. *30th Annual Conference on Physical Electronics*, Milwaukee, d2:60.
47. Hoffman, W.R., 1966. *Physics of Thin Films*, 3:211.
48. Sasabe, H., S. Saito, M. Asahina and H. Kakutani, 1969. *Journal of Polymer Science*, Part A-2, 7:1405-1414.
49. Yokohama, S., D.W. Dong, D.J. DiMaria, S.K. Lai, 1983. *Journal of Applied Physics*, 54:7058-7065.
50. Berry, B.S., 1978. *Metallic Glasses*. Metals Park, OH: ASM, pp. 161-189.
51. Hussain, A.A. and J.S.S. Whiting, 1985. *Journal of Physics E (Scientific Instruments)*, 18:574-576.
52. Arora, V.K. and K.N. Chopra, 1997. *Thin Solid Films*, 304:24-27.
53. Noyan, I.C., T.C. Huang and B.R. York, 1995. *Critical Reviews in Solid State and Materials Sciences*, 20(2):125-177.
54. New Spectra, 1983. *New Optical Monitoring System Measures Thickness More Precisely and More Easily*. Photonics Spectra, 18.
55. *Laser Extensometer 3000*. Application Note, Optrax Inc, Beverly, MA
56. Wolff, E.G., 1995. *Proceedings ITES-XI*, Pittsburgh; also Norris, M.A., D.J. Oakes and E.G. Wolff, 1995. *SAMPE Sympos. Proc.* 40:1855.
57. Saenger, K.L. and H.M. Tong, 1990. *New Characterization Techniques for Thin Polymer Films*. H.M. Tong and L. Nguyen, eds. New York: Wiley-Interscience.
58. Nedorezov, S.S., 1971. *Soviet Physics - JETP*, 32:739.